Electronic Supplementary Material (ESI) for Physical Chemistry Chemical Physics

Supporting Information

The molecular clusters in a supercritical fluid-solid system should be considered as a phase — thermodynamic principle and evidence

Minqiang Hou, Jianling Zhang, Buxing Han,* Qingqing Mei, Hui Ning, Dezhong Yang

CAS Key Laboratory of Colloid, Interface and Chemical Thermodynamics, Beijing National Laboratory for Molecular Sciences, Institute of Chemistry, Chinese Academy of Sciences

Fax: 86-10-62562821; E-mail: *hanbx@iccas.ac.cn* (Buxing Han)

This file includes:

1. Experimental

1.1 Materials

Aspirin (meets USP testing specifications), Benzoic acid (ACS reagent, ≥99.5%), Biphenyl (99.5%), Flouranthene (98%), Phenanthrene (98%), naphthalene (99%),

were obtained from Sigma-Aldrich, USA. The acetone, ethanol, acetonitrile, and n-pentane were purchased from Beijing Chemical Reagent Factory, which were all analytical grade. The chemicals were used without further purification. The CO_2 with a purity of 99.99% was provided from Beijing Analytical Instrument Factory.

1.2 Apparatus

The supercritical fluid (SCF)-solid equilibrium data were determined by static method[S1] using the apparatus used previously[S2]. The apparatus consisted mainly of a high-pressure variable-volume view cell, a constant temperature water bath, a high-pressure pump, a pressure gauge, a magnetic stirrer, and a sample bomb. The high-pressure view cell was composed of a stainless steel body, a stainless steel piston, and two quartz windows. The piston in the view cell could be moved up and down, so that the volume of the view cell could be changed in the range from 20 to 50 cm^3. The apparatus could be used up to 20 MPa. The view cell was immersed in constant temperature water bath that was controlled using a Haake-D8 temperature controller. The temperature was measured by an accurate mercury thermometer with an accuracy of better than ±0.05 K. The pressure gauge was composed of a pressure transducer (Model FOXBORO/ICT) and a pressure indicator. It was accurate to ±0.025 MPa in the pressure range.

1.3 Experimental procedures

The experimental procedures were also similar to those used previously[S2]. We describe the procedures to determine the solubility of a solute in SC CO_2 with cosolvent in detail because those without cosolvent were similar and simpler. In a typical experiment, a suitable amount of solute was loaded into the view cell, and the air in the view cell was removed by vacuum. The CO_2/cosolvent mixture of desired composition was charged into the view cell by a stainless steel sample bomb. The amount of CO_2/cosolvent mixture added was known by weighing the sample bomb before and after filling the view cell. The mole fractions of the components in the view cell could be known easily from their masses of the components in the system.

The view cell was placed in the constant temperature bath. After thermal equilibrium was reached, the system pressure was increased slowly by moving the piston down until all the solid solute was dissolved completely, and the pressure was recorded. At this pressure, some solute precipitated after slight reduction in pressure, indicating that the pressure was the saturation pressure. The procedures to determine the solubility of a solute in pure CO_2 were similar. The main difference was that pure CO_2 was used instead of CO_2/cosolvent mixture. It was estimated that the accuracy of solubility data determined was better than ±2%.

The solubility of naphthalene in supercritical (SC) CO_2 has been determined by different researchers. The reliability of the apparatus and experimental procedures of this work were tested by determining the solubility of naphthalene in SC CO_2. The comparison of the results determined in this work and those reported in the literature [S3, S4] is illustrated in Fig. S1. Obviously, the data determined in this work agree well with those reported by other authors.

2. Calculation methods

The SCF-solid phase equilibria of different systems were calculated using the principle proposed in this work (Scheme 1 B) by combination of the Monte Carlo simulation and PR-EOS. The block diagram is shown in Fig. 1, and the calculation steps are described briefly in the main text. The calculation methods and procedures are discussed in the following.

2.1 Calculation of the fugacity of the solute in the solid phase

The fugacity of the solute in the solid phase f_{solute}^{S}, the first term of Equation (1), is calculated by Equation (S1) [S5].

$$f_{solute}^{S} = P_{solute}^{sat}\varphi_{solute}^{sat}\exp[v_{solute}^{solid}(P - P_{solute}^{sat})/RT] \qquad \text{(S1)}$$

where P_{solute}^{sat}, φ_{solute}^{sat}, and v_{solute}^{solid} denote the saturation vapor pressure of the pure solid, fugacity coefficient of the solid at saturation pressure P_{solute}^{sat}, and the molar volume of

the solid solute, respectively. φ_{solute}^{sat} is usually assumed to be unity [S5]. The saturation vapor pressures and molar volumes of the solid solutes used in the calculation are from the literature and are listed in Table S1.

2. Monte Carlo simulation

In this work, the size and composition of the clusters in the systems are required, which are function of many factors, such as temperature, pressure, nature of the components, overall composition, surface effect, intermolecular interaction. In this work, Monte Carlo simulation was used to get the properties of the clusters, which is a commonly used method.

Calculation of the radial distribution functions (RDFs) Radial distribution function, $g_{ij}(r)$, describes the probability of finding a particle in the distance r from another particle, relative to the probability expected for a completely random distribution at the same density[S6]. In this work, Monte Carlo simulation was performed in the *NPT* ensemble with periodic boundary condition[S6-S8]. The standard Metropolis method [S9] was used to obtain new configurations under the *NPT* ensemble. The *Lennard-Jones* type potentials[S10] were used to calculate the potential energy between two given molecules, i and j:

$$u_{ij}(r) = 4\varepsilon_{ij}[(\frac{\sigma_{ij}}{r})^{12} - (\frac{\sigma_{ij}}{r})^{6}] \qquad \text{(S2)}$$

where u_{ij} is the pair wise interaction. ε_{ij} and σ_{ij} are the energy parameter and distance parameter, respectively, and i, j=1, 2, 3; 1, 2 and 3 denote the solute, cosolvent, and SC solvent, respectively. The cross-term Lennard-Jones parameters between different molecules were calculated according to the Lorentz-Berthelot mixing rules [S11].

$$\varepsilon_{ij} = \sqrt{\varepsilon_{ii}\varepsilon_{jj}} \qquad \text{(S3)}$$

$$\sigma_{ij} = \frac{1}{2}(\sigma_{ii} + \sigma_{jj}) \qquad \text{(S4)}$$

A spherical cutoff radius of half-length of the box was taken and the tail corrections were applied to correct for this truncation. For each simulation, the system

started from random distribution configurations.

The Lennard-Jones potential parameters of the solute molecules were calculated using the corresponding state principle, which assures that all Lennard-Jones fluids for pure components obey the same reduced equation of state by using the reduced variables:

$$P^* = P\sigma^3/\varepsilon, T^* = kT/\varepsilon \quad \text{(S5)}$$

where P, T, and k stand for pressure, absolute temperature, and Boltzmann constant, respectively, and * denotes the reduced properties. The T* and P* at the critical point are 1.35 and 0.1418, respectively[S11, S12]. The critical constants of the chemicals involved are from the handbook by Poling *et al.*[S13]. The Lennard-Jones parameters used in the simulation are presented in Table S2.

The solute was considered as the center in the simulation. The simulation was performed at fixed temperature, pressure, total number of molecules (N), and composition. Equilibrium was established after approximately 1×10^8 moves, simulation averages were accumulated for approximately 2×10^8 moves.

An example to calculate the RDFs As an example, we discuss the detailed procedures to calculate the solubility of naphthalene in CO_2 with 2.5 mol% n-pentane at 308.15 K and 8.3 MPa. In the Monte Carlo simulation, the total number of molecules N was 100000. Firstly, the solubility of naphthalene in the CO_2+n-pentane (2.5 mol%) mixed solvent was assumed to be 0.01. So the numbers of CO_2, n-pentane and naphthalene in the fluid are 96525, 2475 and 1000, respectively. Monte Carlo simulation was performed in the *NPT* ensemble with periodic boundary condition. Equilibrium was established after approximately 1×10^8 moves, simulation averages were accumulated for approximately 2×10^8 moves. For the *NPT* ensemble, volume of the box was changed once every 100000 cycles in this work. The system started from random distribution configurations. Fig. S2 shows the RDFs of the CO_2+n-pentane +naphthalene system at the temperature, pressure, and composition.

Calculation of the mole fractions of the components in the clusters The mole fractions of the components in the clusters were calculated using equations

(S6)-(S7)[S14].

$$N_j^C = 4\pi \frac{N_j}{V} \int_0^L g_{ij}(r) r^2 dr \qquad \text{(S6)}$$

$$y_j^C = N_j^C / \sum_j N_j^C \qquad \text{(S7)}$$

where N_j stands for the number of the component j in the fluid (N_{solute}, $N_{cosolvent}$, $N_{solvent}$), N_j^C the number of the component j in a cluster, y_j^C the mole fraction of component j in a cluster (y_{solute}^C, $y_{cosolvent}^C$, $y_{solvent}^C$). The integration limit L was the distance of the first minimum of the radial distribution function g_{ii}(r), similar to that used by many other authors [S15, S16].

Calculation of the mole fractions of the components in the bulk phase The mole fractions of the component in the bulk phase can be calculated easily by the equations (S8) and (S9).

$$N_j^B = N_j - n_{cluster} N_{ij}(L) \qquad \text{(S8)}$$

$$y_j^B = N_j^B / \sum_j N_j^B \qquad \text{(S9)}$$

where y_j^B is the mole fraction of a component in the bulk phase (y_{solute}^B, $y_{cosolvent}^B$, $y_{solvent}^B$), N_j^B is the number of the component j in bulk phase.

3. Calculation of fugacities of the components by equation of state

To get the fugacities of the components, the fugacity coefficients are required as shown in equations 1-3. It is known that the fugacity coefficients of the components in a system depend on many factors, including temperature, pressure, intermolecular interaction, surface effect, and so on. In this work, the fugacity coefficients were calculated using Peng-Robinson equation of state, which is a widely used method. The equation of state method is predictive in the sense of two reasons. First, using the binary interaction coefficient k_{ij} of a binary system obtained from a few experimental phase equilibrium data, one can predict the phase equilibrium data at all other conditions where the experimental data are not available. For example, using the k_{ij} obtained at one temperature, we can predict the data at other temperatures. Second,

using the interaction coefficients obtained from the related binary systems, one can predict the phase equilibrium data of multicomponent systems, such as ternary, quaternary systems.

Calculation of the fugacity coefficients of the components in different phases

Peng-Robinson equation of state (PR-EOS) is a commonly used method to calculate the fugacity coefficients of the components in different systems [S17, S18], which can be expressed as follow.

$$P = \frac{RT}{V-b} - \frac{a}{V(V+b)+b(V-b)} \qquad \text{(S10)}$$

$$a = 0.457235\frac{R^2 T_c^{\ 2}}{P_c}\alpha \qquad \text{(S11)}$$

$$b = 0.077796 RT_c / P_c \qquad \text{(S12)}$$

$$\alpha = [1 + m(1-\sqrt{T/T_C})]^2 \qquad \text{(S13)}$$

$$m = 0.37464 + 1.54226\omega - 0.26992\omega^2 \qquad \text{(S14)}$$

For a mixture, the following van der Waals mixing rules are applied.

$$a = \sum_i \sum_j y_i y_j a_{ij} \qquad \text{(S15)}$$

$$b = \sum_i y_i b_i \qquad \text{(S16)}$$

$$a_{ij} = (1-k_{ij})\sqrt{a_i a_j} \qquad \text{(S17)}$$

where T_c, P_c, and ω stand for the critical temperature, critical pressure, and acentric factor, respectively; P, V, T and R are pressure, molar volume, absolute temperature and gas constant, respectively. The k_{ij} is the binary interaction coefficients. Based on the PR-EOS and the mixing rules, the fugacity coefficient of each component can be calculated by following equation [S17, S19].

$$\ln\varphi_i = \frac{b_i}{b}\left(\frac{PV}{RT}-1\right) - \ln\left[\frac{PV}{RT}\left(1-\frac{b}{V}\right)\right] - \frac{a}{2\sqrt{2}bRT}\left(\frac{2\sum_j y_j a_{ij}}{a} - \frac{b_i}{b}\right)\ln\left(\frac{V+2.414b}{V-0.414b}\right) \qquad \text{(S18)}$$

The critical temperatures, critical pressures, and acentric factors of the components used in the calculation are given in Table S2. The binary interaction

coefficients are presented in Table S3, which were obtained by correlation the experimental data using conventional principle, *i.e.*, Scheme 1A.

Calculation of the fugacities After the fugacity coefficients and mole fractions of the components have been calculated as discussed above, the fugacities of the solute, cosolvent, and solvent in the cluster phase and bulk phase can be easily calculated by following equations.

$$f_{solute}^{C} = \varphi_{solute}^{C} y_{solute}^{C} P \qquad \text{(S19)}$$

$$f_{solute}^{B} = \varphi_{solute}^{B} y_{solute}^{B} P \qquad \text{(S20)}$$

$$f_{cosolvent}^{C} = \varphi_{cosolvent}^{C} y_{cosolvent}^{C} P \qquad \text{(S21)}$$

$$f_{cosolvent}^{B} = \varphi_{cosolvent}^{B} y_{cosolvent}^{B} P \qquad \text{(S22)}$$

$$f_{solvent}^{C} = \varphi_{solvent}^{C} y_{solvent}^{C} P \qquad \text{(S23)}$$

$$f_{solvent}^{B} = \varphi_{solvent}^{B} y_{solvent}^{B} P \qquad \text{(S24)}$$

4. Results

The phase equilibrium data of the systems were calculated from PR-EOS by conventional principle (Scheme 1A) and present principle using the same parameters listed in Table S3, and the results are all demonstrated in Figures 2-5 and Figures S3-S19 for comparison.

The degree of clustering (DC), which is defined as the ratio of the number of the molecules in the cluster phase ($\sum N_j^C$) and the total number of the molecules in the fluid (N), obtained from the Monte Carlo simulation are given in Figures S20-S40. The general trend is that the degree of clustering is larger near the critical region of the SC solvents, and smaller at the conditions far from the critical region, which is consistent with the conclusion reported in the literature.

It can be known by comparing the calculated phase equilibrium data (Figures 2-5, Figures S3-S19) and the results of degree of clustering (Figures S20-S40) that the

phase equilibrium data calculated by the present principle are more consistent with the experimental results than those calculated from the conventional principle near the critical region of the solvents where the degree of clustering is large.

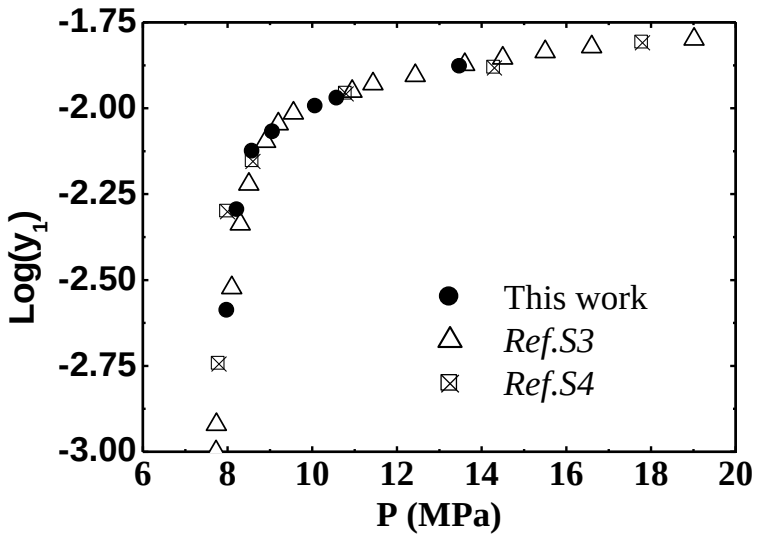

Fig. S1 The solubility of naphthalene in SC CO_2 at 308.15 K determined by different authors.

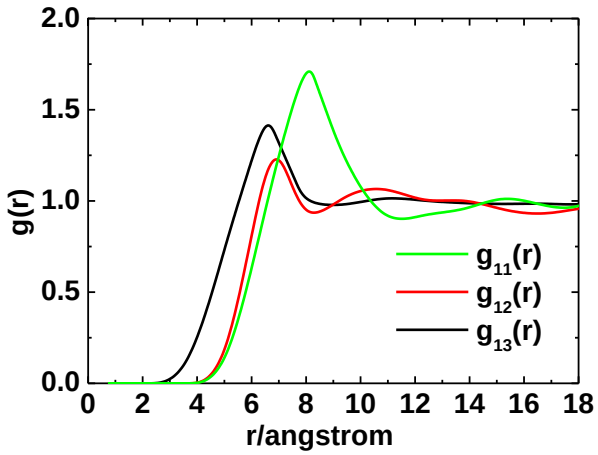

Fig. S2 RDFs of naphthalene(1) + n-pentane(2) + CO_2(3) system at 308.15 K and 8.3 MPa. The mole fraction of n-pentane in CO_2 + n-pentane mixture is 0.025.

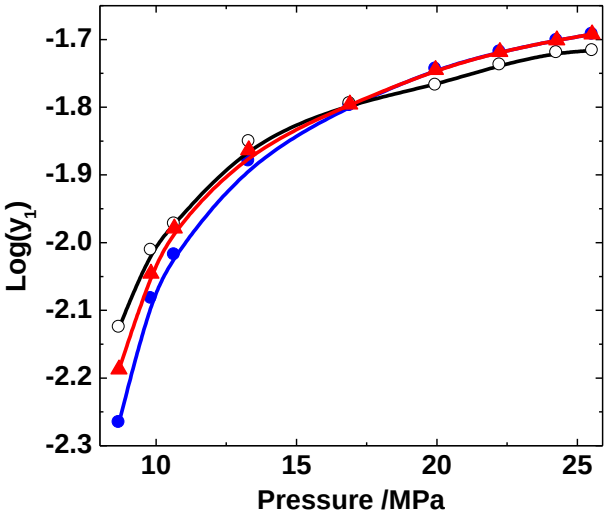

Fig. S3 The solubility of naphthalene in SC CO_2 at 308.15 K and different pressures. ○The experimental results (Ref. S6); ▲the results calculated by the principle of this work; ●the results calculated by the conventional principle using the same equation of state.

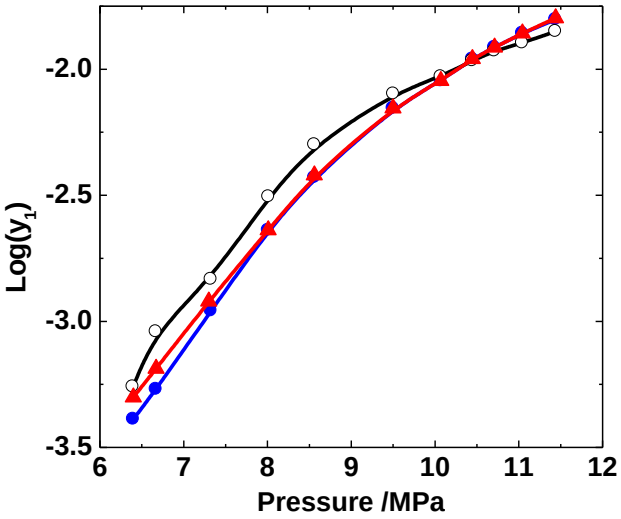

Fig. S4 The solubility of naphthalene in SC ethylene at 308.15 K and different pressures. ○The experimental results (Ref. S20); ▲the results calculated by the principle of this work; ●the results calculated by the conventional principle using the same equation of state.

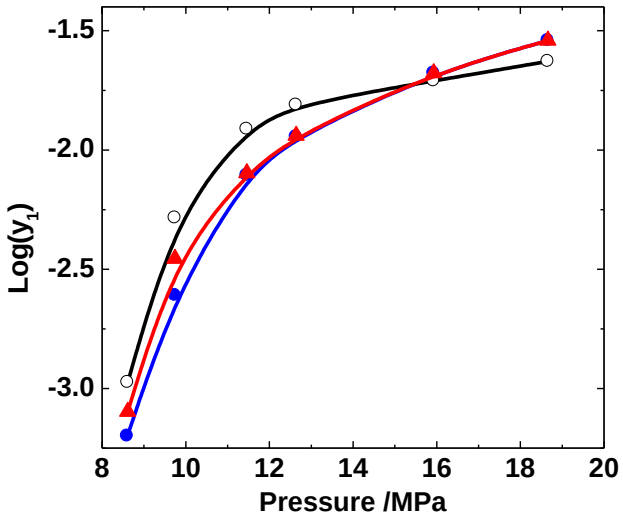

Fig. S5 The solubility of p-quinone in SC CO_2 at 318.15 K and different pressures. ○The experimental results (Ref. S21); ▲the results calculated by the principle of this work; ●the results calculated by the conventional principle using the same equation of state.

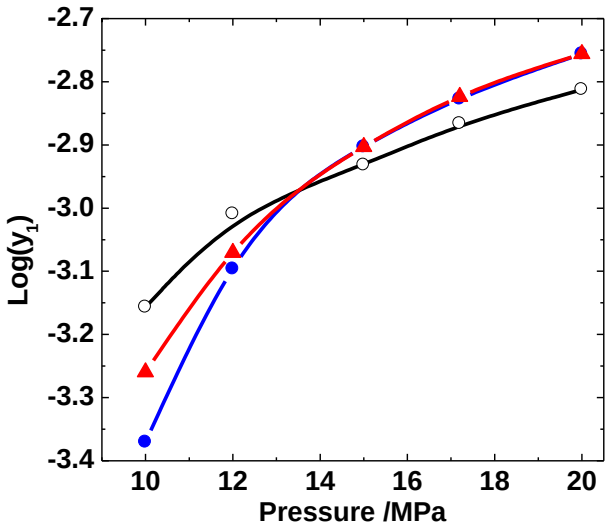

Fig. S6 The solubility of aspirin in SC CO_2+methanol (y_2=0.03) mixture at 318.15 K and different pressures. ○ The experimental results (Ref. S22); ▲ the results calculated by the principle of this work; ● the results calculated by the conventional principle using the same equation of state.

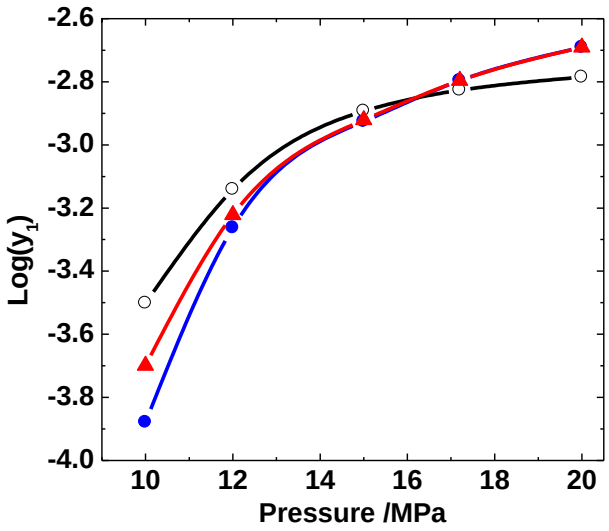

Fig. S7 The solubility of aspirin in SC CO_2+ethanol (y_2=0.03) mixtures at 328.15 K. ○The experiment results (Ref. S22); ▲the results calculated by the principle of this work; ●the results calculated by the conventional principle using the same equation of state.

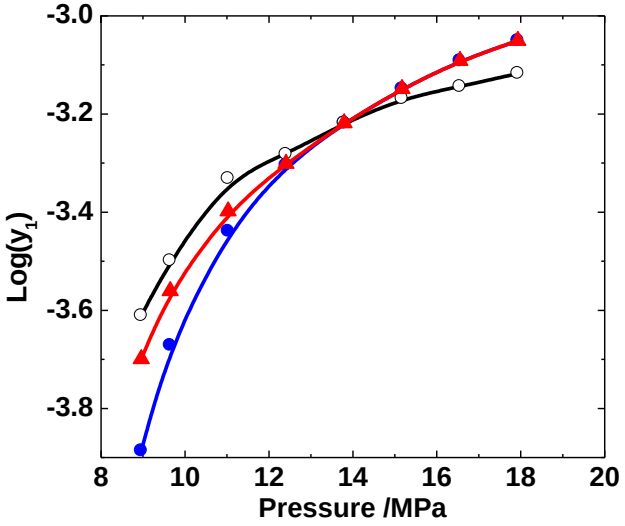

Fig. S8 The solubility of naproxen in SC CO_2+acetone (y_2=0.035) mixture at 318.15 K and different pressures. ○The experimental results (Ref. S23); ▲the results calculated by the principle of this work; ●the results calculated by the conventional principle using the same equation of state.

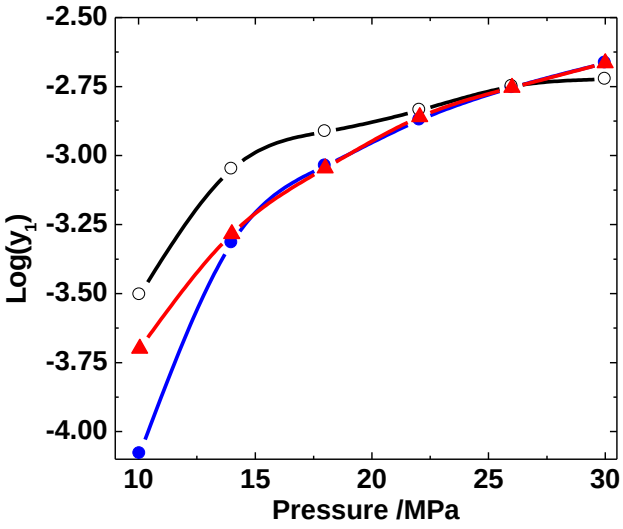

Fig. S9 The solubility of 2-naphthol in SC CO_2+cyclohexane (y_2=0.036) mixture at 328.15 K and different pressures. ○The experimental results (Ref. S24) ; ▲the results calculated by the principle of this work; ●the results calculated by the conventional principle using the same equation of state.

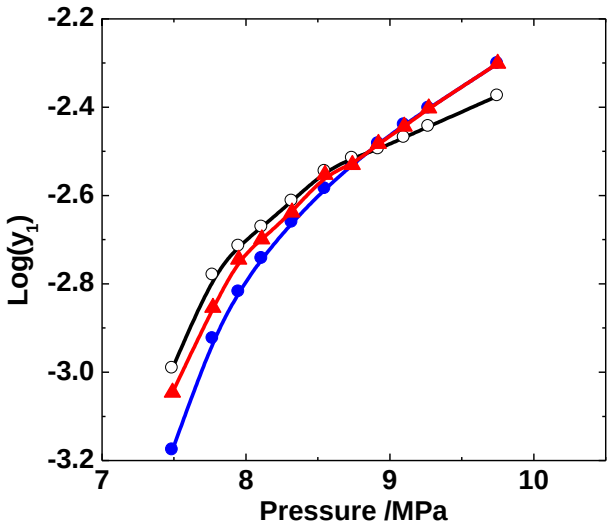

Fig. S10 The solubility of 1, 4-naphthoquinone in SC CO_2+n-pentane (y_2=0.021) mixture at 308.15 K and different pressures. ○The experimental results (Ref. S25) ; ▲the results calculated by the principle of this work; ●the results calculated by the conventional principle using the same equation of state.

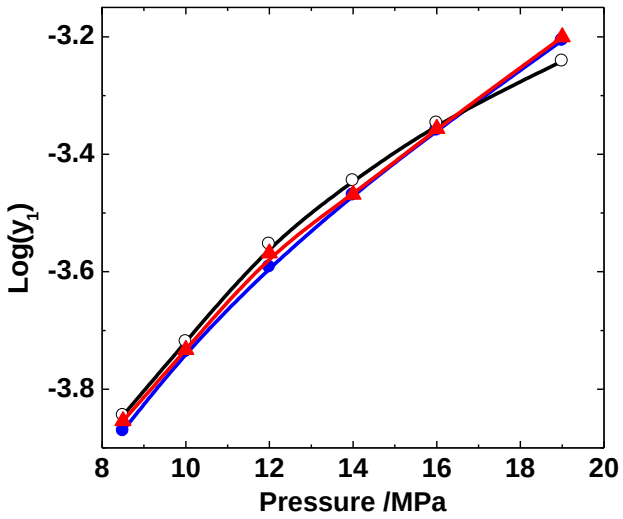

Fig. S11 The solubility of cholesterol in SC ethane+propane (y_2=0.14) mixture at 318.15 K and different pressures. ○The experimental results (Ref. S26); ▲the results calculated by the principle of this work; ●the results calculated by the conventional principle using the same equation of state. The critical pressures studied are much higher than the critical pressure of ethane (4.872 MPa) and the clustering in the system is not considerable. Therefore, the results calculated by the two principles are similar.

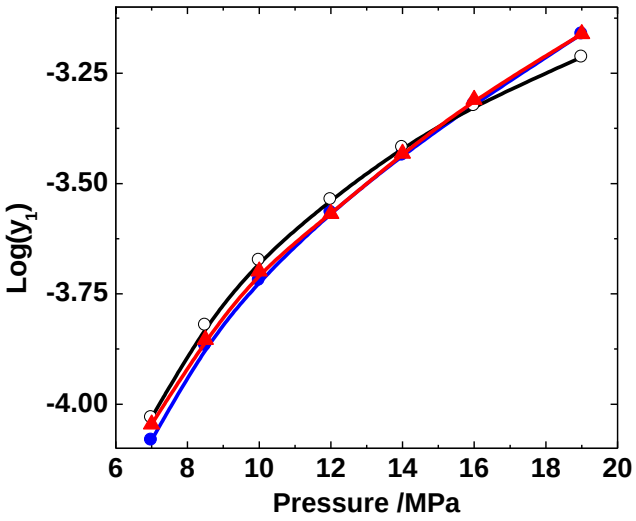

Fig. S12 The solubility of Cholesterol in SC ethane + acetone (y_2=0.035) mixture at 318.15 K and different pressures. ○, The experimental results (Ref. S27) ; ▲the results calculated by the principle of this work; ●the results calculated by the conventional principle using the same equation of state.

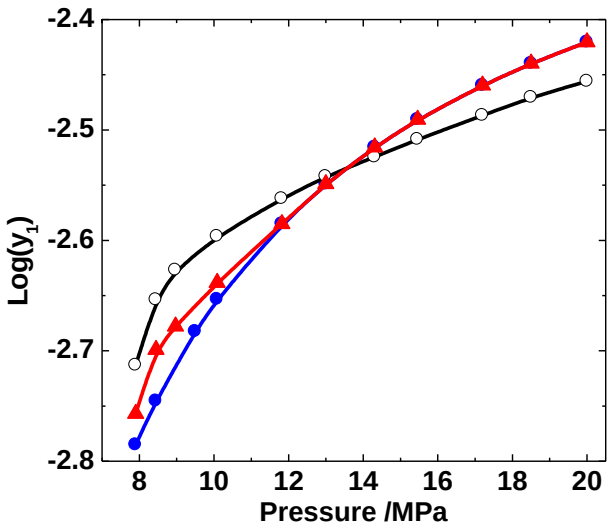

Fig. S13 The solubility of aspirin in SC CO_2 + ethanol (y_2=0.05) mixture at 308.15 K and different pressures. ○The experimental results of this work; ▲the results calculated by the principle of this work; ●the results calculated by the conventional principle using the same equation of state.

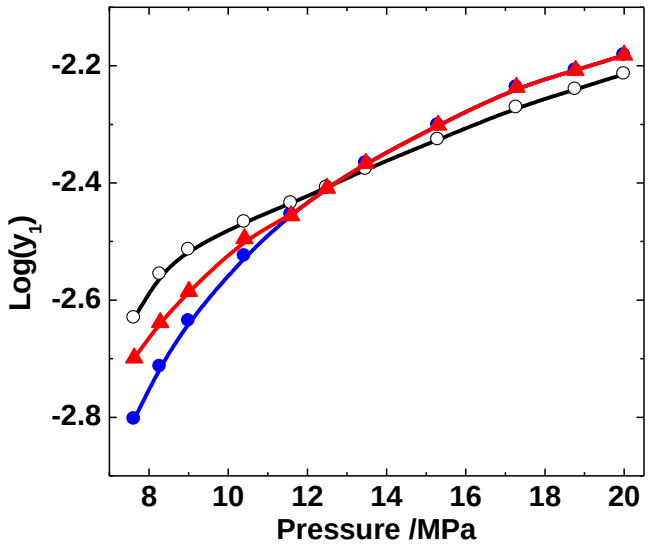

Fig. S14 The solubility of benzoic acid in SC CO_2 + acetonitrile (y_2=0.04) mixture at 308.15 K and different pressures. ○The experimental results of this work; ▲the results calculated by the principle of this work; ●the results calculated by the conventional principle using the same equation of state.

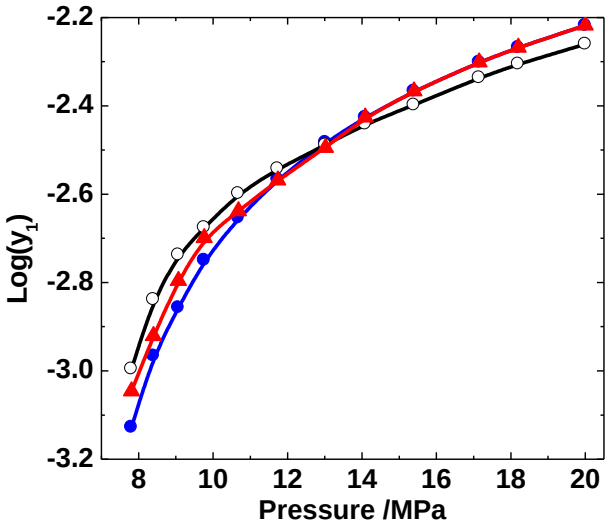

Fig. S15 The solubility of benzoic acid in SC CO_2 + n-pentane (y_2=0.03) mixture at 308.15 K and different pressures. ○The experimental results of this work; ▲the results calculated by the principle of this work; ●the results calculated by the conventional principle using the same equation of state.

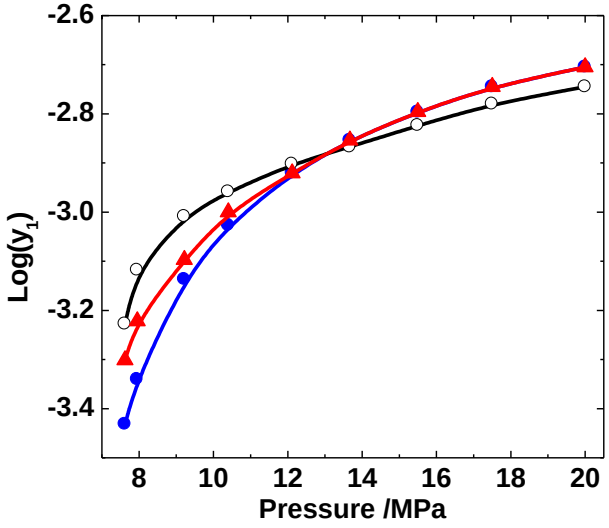

Fig. S16 The solubility of phenanthrene in SC CO_2 + n-pentane (y_2=0.035) mixture at 308.15 K and different pressures. ○The experimental results of this work; ▲the results calculated by the principle of this work; ●the results calculated by the conventional principle using the same equation of state.

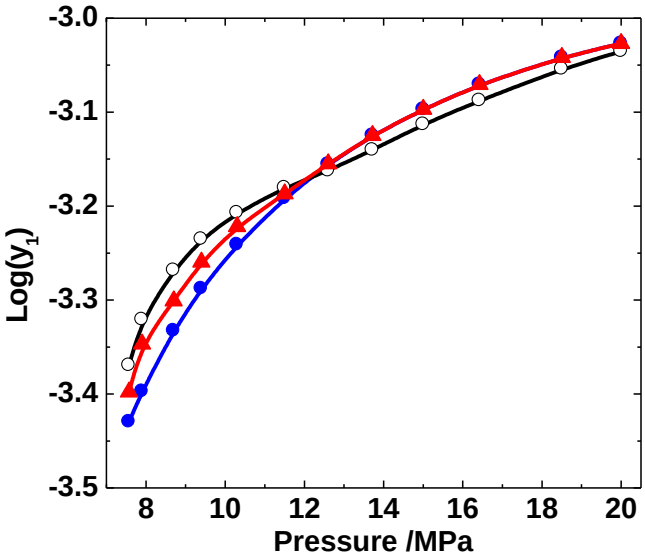

Fig. S17 The solubility of flouranthene in SC CO_2 + acetone (y_2=0.05) mixture at 308.15 K and different pressures. ○The experimental results of this work; ▲the results calculated by the principle of this work; ●the results calculated by the conventional principle using the same equation of state.

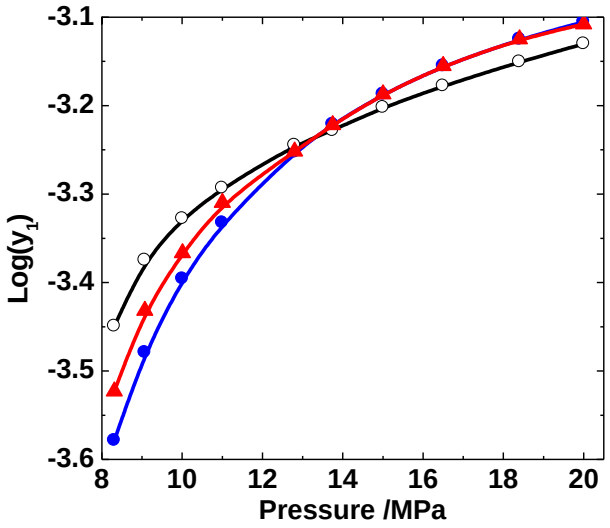

Fig. S18 The solubility of flouranthene in SC CO_2 + n-pentane (y_2=0.05) mixture at 308.15 K and different pressures. ○The experimental results of this work; ▲the results calculated by the principle of this work; ●the results calculated by the conventional principle using the same equation of state.

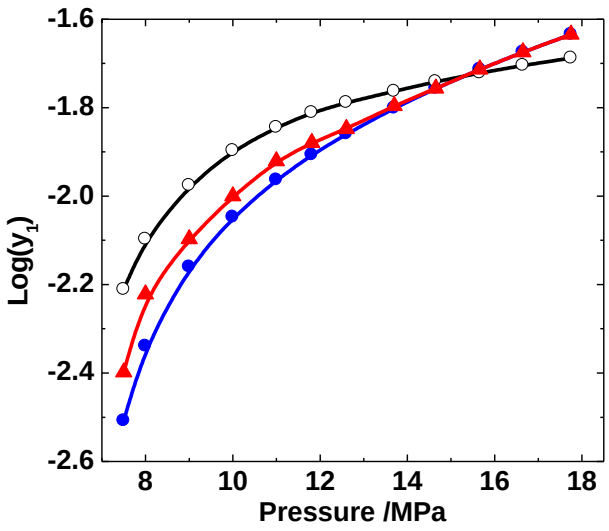

Fig. S19 The solubility of bipheny in SC CO_2 + n-pentane (y_2=0.025) mixture at 308.15 K and different pressures. ○The experimental results of this work; ▲the results calculated by the principle of this work; ●the results calculated by the conventional principle using the same equation of state.

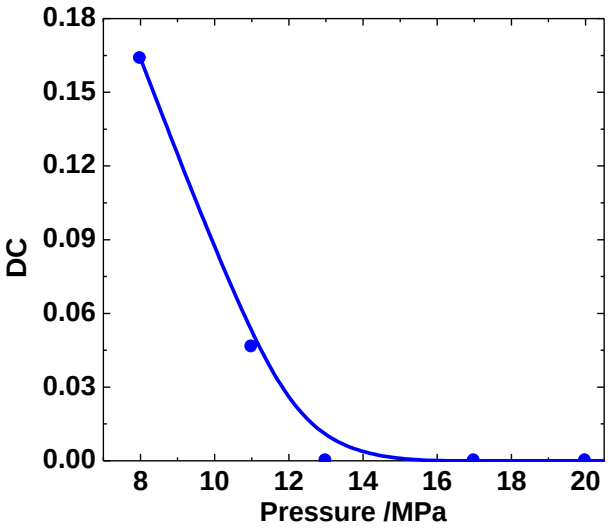

Fig. S20. The degree of clustering (DC, the ratio of the number of the molecules in the cluster phase and the total number of the molecules in the fluid) of benzoic acid + ethyl acetate (y_2=0.02) + SC CO_2 system at 328.15 K and different pressures and at the equilibrium condition.

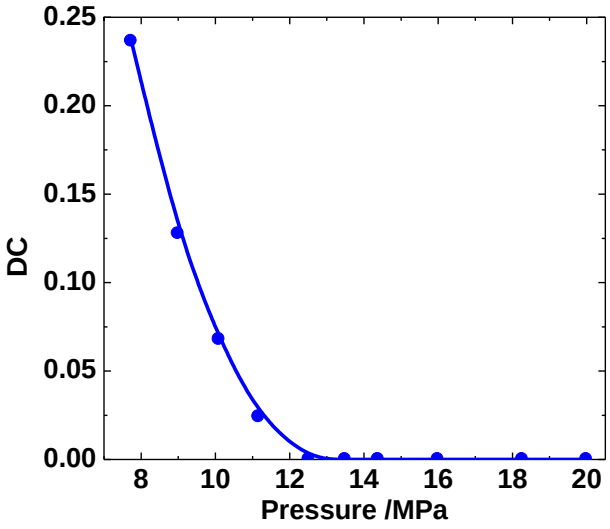

Fig. S21. The degree of clustering (DC, the ratio of the number of the molecules in the cluster phase and the total number of the molecules in the fluid) of phenanthrene + acetone (y_2=0.035) +SC CO_2 system at 308.15 K and different pressures and at the equilibrium condition.

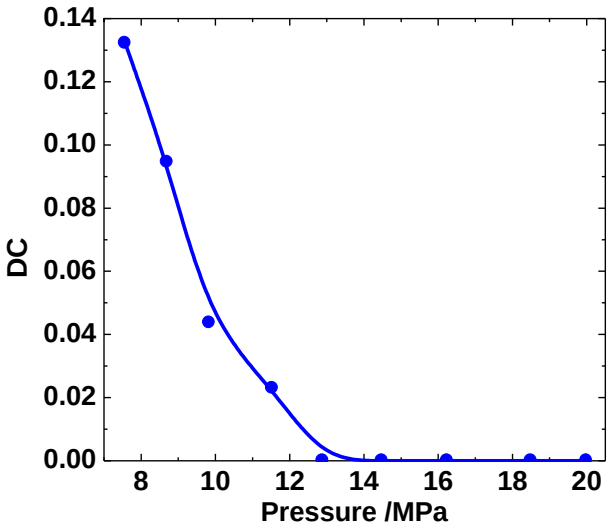

Fig. S22. The degree of clustering (DC, the ratio of the number of the molecules in the cluster phase and the total number of the molecules in the fluid) of aspirin + acetone (y_2=0.04) + SC CO_2 system at 308.15 K and different pressures and at the equilibrium condition.

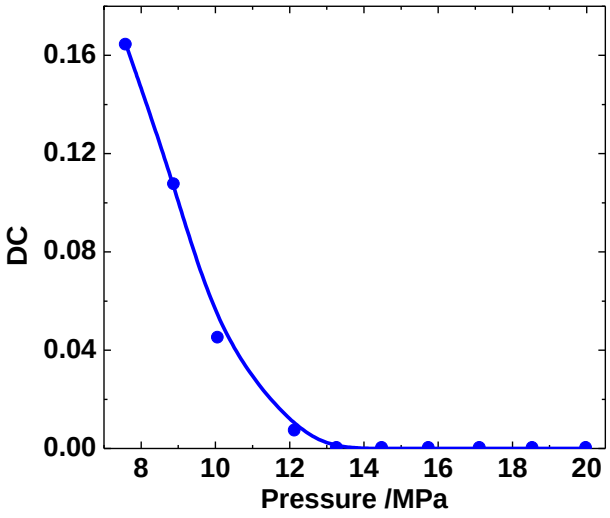

Fig. S23. The degree of clustering (DC, the ratio of the number of the molecules in the cluster phase and the total number of the molecules in the fluid) of naphthalene + n-pentane (y_2=0.025) + SC CO_2 system at 308.15 K and different pressures and at the equilibrium condition.

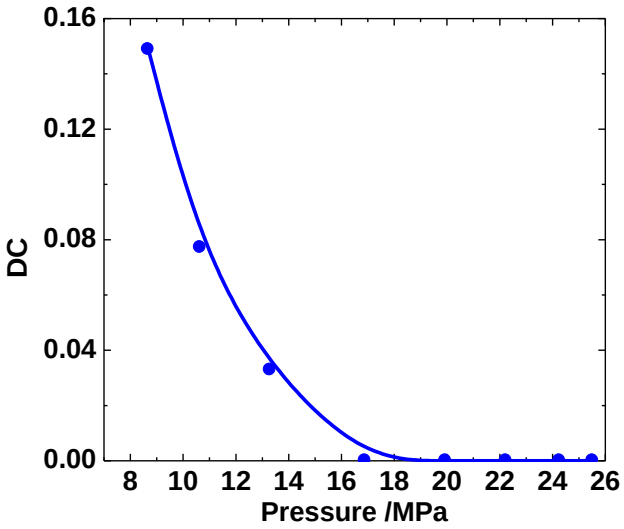

Fig. S24. The degree of clustering (DC, the ratio of the number of the molecules in the cluster phase and the total number of the molecules in the fluid) of naphthalene + SC CO_2 system at 308.15 K and different pressures and at the equilibrium condition.

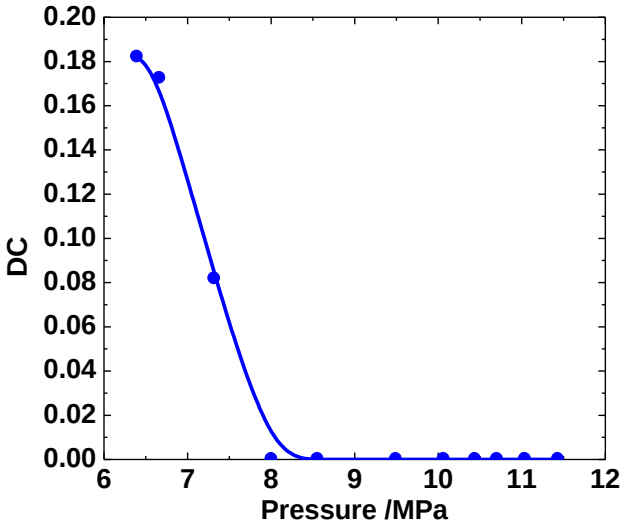

Fig. S25. The degree of clustering (DC, the ratio of the number of the molecules in the cluster phase and the total number of the molecules in the fluid) of naphthalene + SC ethylene system at 308.15 K and different pressures and at the equilibrium condition.

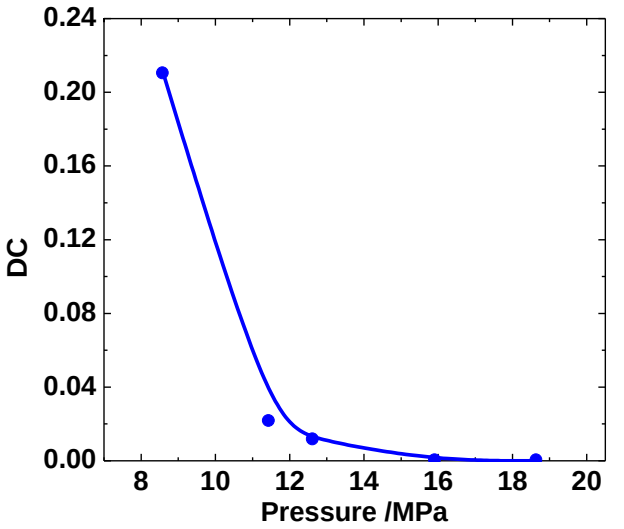

Fig. S26. The degree of clustering (DC, the ratio of the number of the molecules in the cluster phase and the total number of the molecules in the fluid) of p-quinone + SC CO_2 system at 308.15 K and different pressures and at the equilibrium condition.

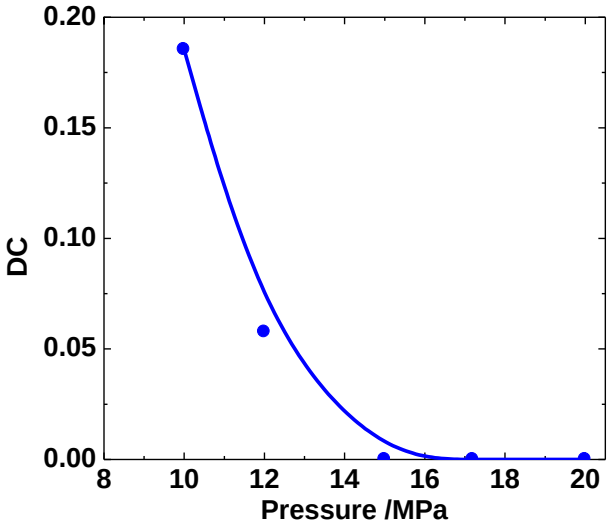

Fig. S27. The degree of clustering (DC, the ratio of the number of the molecules in the cluster phase and the total number of the molecules in the fluid) of aspirin + methanol (y_2=0.03) + SC CO_2 system at 318.15 K and different pressures and at the equilibrium condition.

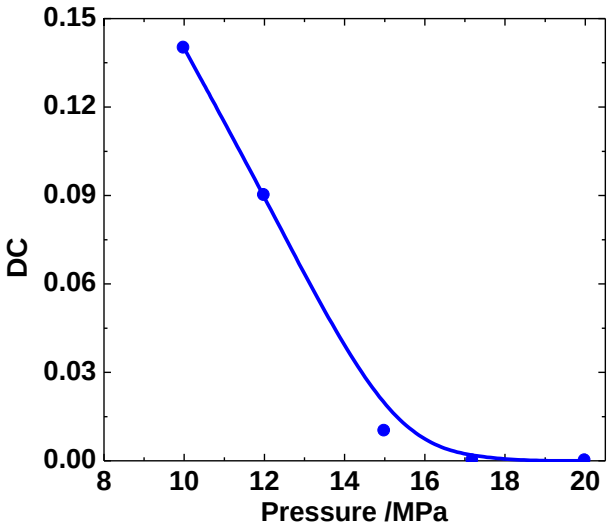

Fig. S28. The degree of clustering (DC, the ratio of the number of the molecules in the cluster phase and the total number of the molecules in the fluid) of aspirin + ethanol (y_2=0.03) + SC CO_2 system at 328.15 K and different pressures and at the equilibrium condition.

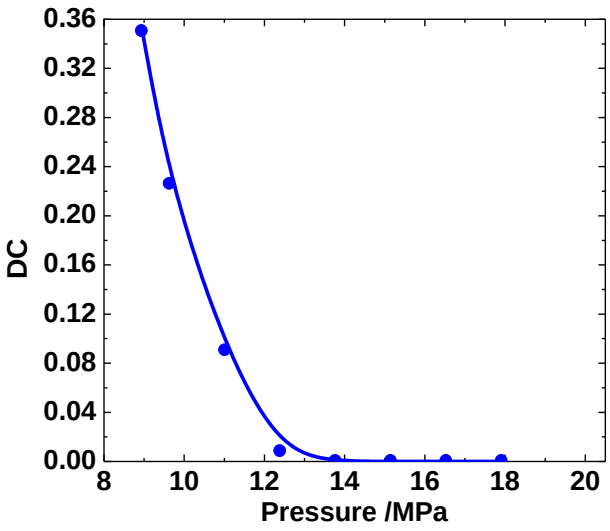

Fig. S29. The degree of clustering (DC, the ratio of the number of the molecules in the cluster phase and the total number of the molecules in the fluid) of naproxen + acetone (y_2=0.035) + SC CO_2 system at 328.15 K and different pressures and at the equilibrium condition.

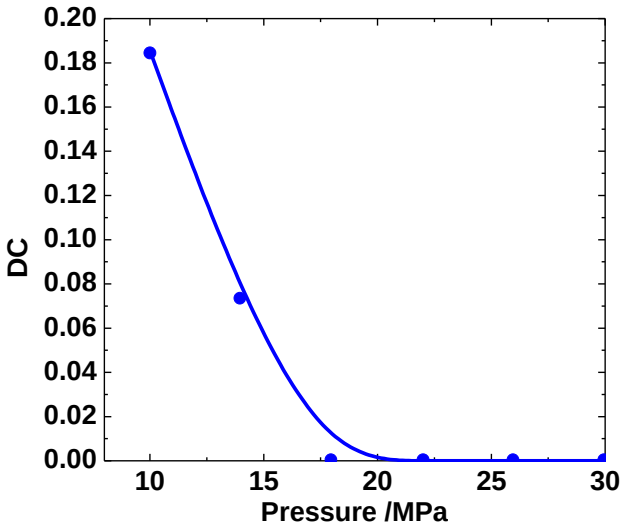

Fig. S30. The degree of clustering (DC, the ratio of the number of the molecules in the cluster phase and the total number of the molecules in the fluid) of 2-naphthol + cyclohexane (y_2=0.036) + SC CO_2 system at 328.15 K and different pressures and at the equilibrium condition.

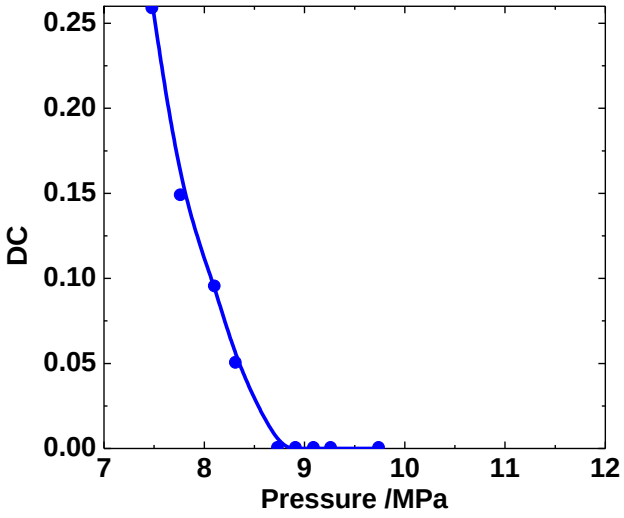

Fig. S31. The degree of clustering (DC, the ratio of the number of the molecules in the cluster phase and the total number of the molecules in the fluid) of 1,4-naphthoquinone + n-pentane (y_2=0.021) + SC CO_2 system at 308.15 K and different pressures and at the equilibrium condition.

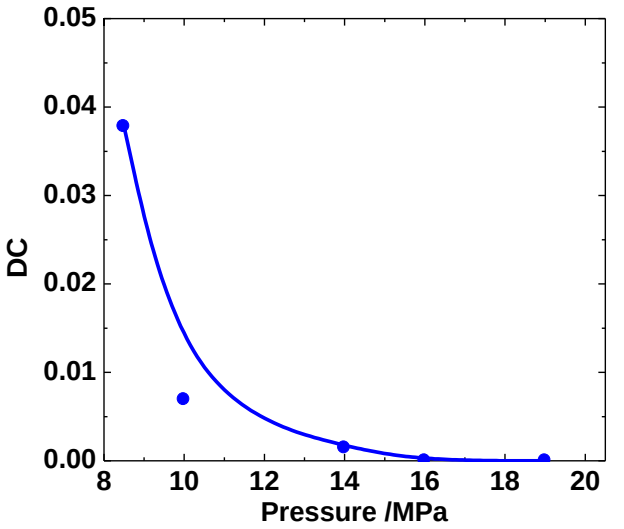

Fig. S32. The degree of clustering (DC, the ratio of the number of the molecules in the cluster phase and the total number of the molecules in the fluid) of cholesterol + propane (y_2=0.14) + SC ethane system at 318.15 K and different pressures and at the equilibrium condition.

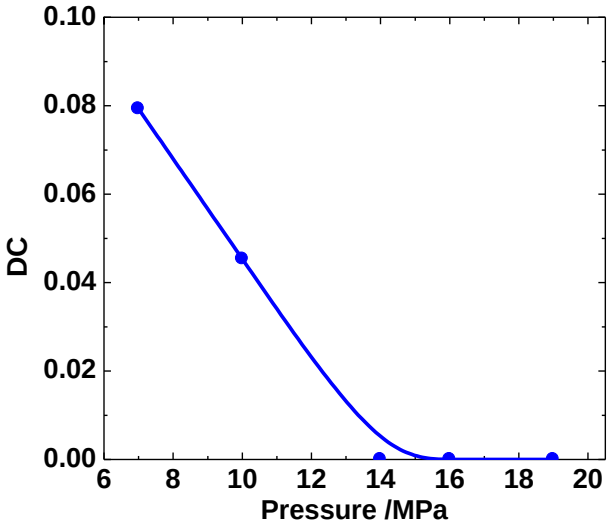

Fig. S33. The degree of clustering (DC, the ratio of the number of the molecules in the cluster phase and the total number of the molecules in the fluid) of cholesterol + acetone (y_2=0.35) + SC ethane system at 318.15 K and different pressures and at the equilibrium condition.

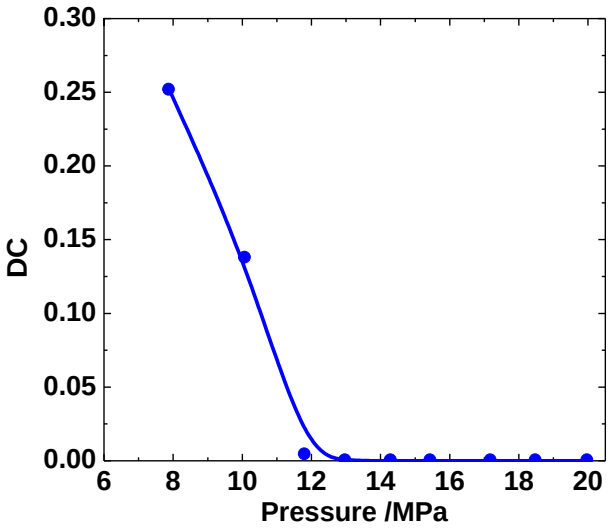

Fig. S34. The degree of clustering (DC, the ratio of the number of the molecules in the cluster phase and the total number of the molecules in the fluid) of aspirin + ethanol (y_2=0.05) + SC CO_2 system at 308.15 K and different pressures and at the equilibrium condition.

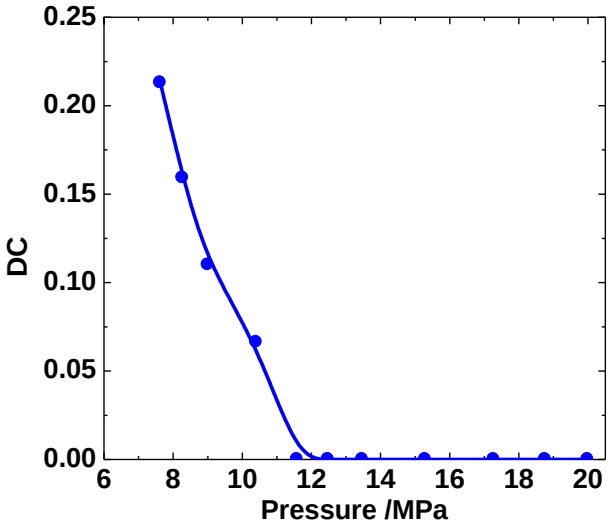

Fig. S35. The degree of clustering (DC, the ratio of the number of the molecules in the cluster phase and the total number of the molecules in the fluid) of benzoic acid + acetonitrile (y_2=0.04) + SC CO_2 system at 308.15 K and different pressures and at the equilibrium condition.

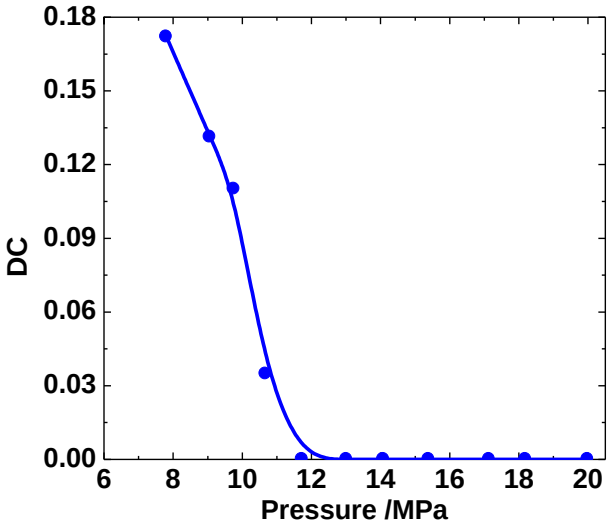

Fig. S36. The degree of clustering (DC, the ratio of the number of the molecules in the cluster phase and the total number of the molecules in the fluid) of benzoic acid + n-pentane (y_2=0.03) + SC CO_2 system at 308.15 K and different pressures and at the equilibrium condition.

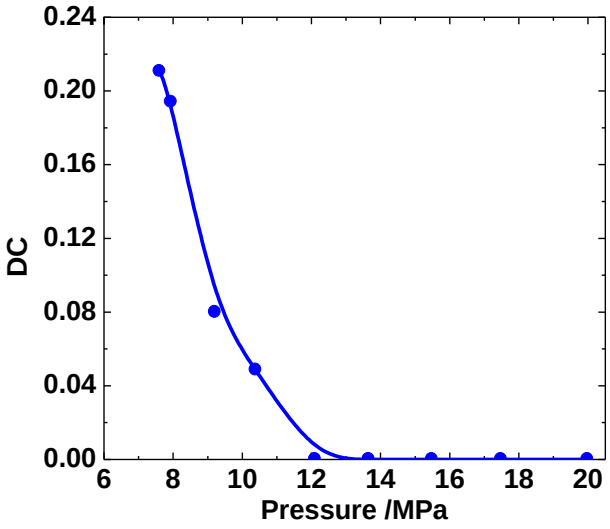

Fig. S37. The degree of clustering (DC, the ratio of the number of the molecules in the cluster phase and the total number of the molecules in the fluid) of phenanthrene + n-pentane (y_2=0.035) + SC CO_2 system at 308.15 K and different pressures and at the equilibrium condition.

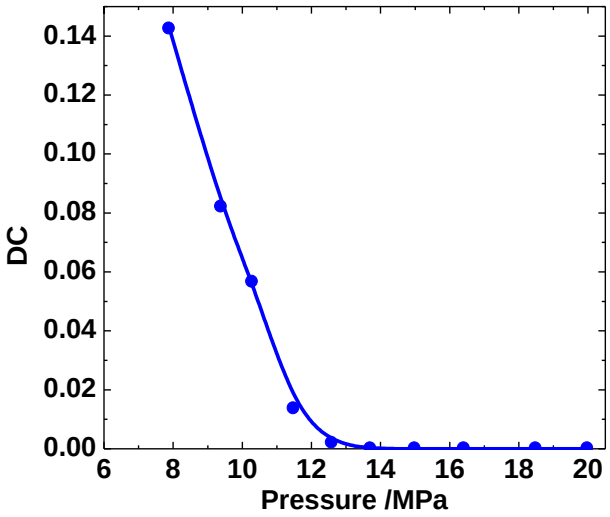

Fig. S38. The degree of clustering (DC, the ratio of the number of the molecules in the cluster phase and the total number of the molecules in the fluid) of flouranthene + acetone (y_2=0.05) + SC CO_2 system at 308.15 K and different pressures and at the equilibrium condition.

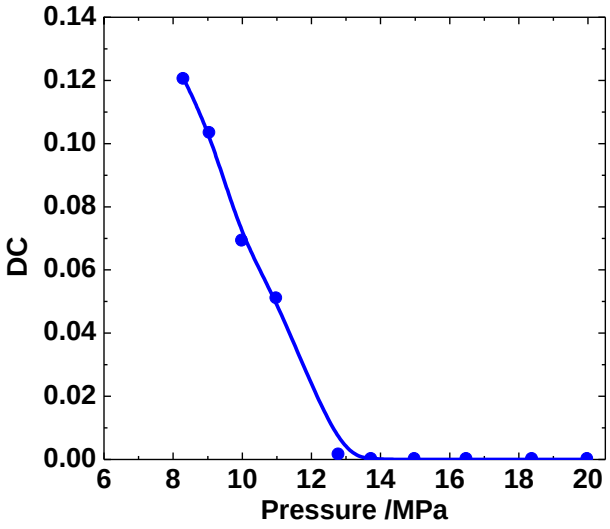

Fig. S39. The degree of clustering (DC, the ratio of the number of the molecules in the cluster phase and the total number of the molecules in the fluid) of flouranthene + n-pentane (y_2=0.05) + SC CO_2 system at 308.15 K and different pressures and at the equilibrium condition.

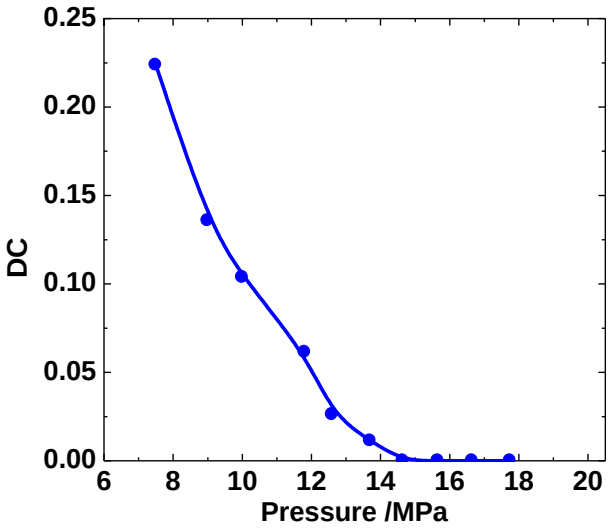

Fig. S40. The degree of clustering (DC, the ratio of the number of the molecules in the cluster phase and the total number of the molecules in the fluid) of biphenyl + n-pentane (y_2=0.025) + SC CO_2 system at 308.15 K and different pressures and at the equilibrium condition.

Table S1 Vapor pressures (P_{sub}) and molar volumes (V_s) of the solutes studied in this work.

System	T (K)	P_{sub} (Pa)	V^s (mL/mol)
Benzoic acid	328.15	3.128[S28]	92.80[S28]
Benzoic acid	308.15	0.37[S28]	92.80[S28]
Naproxen	318.15	0.00637[S29]	178.30[S29]
Aspirin	308.15	0.09021[S30]	129.64[S30]
Aspirin	318.15	0.2803[S30]	129.64[S30]
Aspirin	328.15	0.8011[S30]	129.64[S30]
Flouranthene	308.15	0.00625[S31]	163.0[S31]
Cholesterol	318.15	0.0573[S32]	371.56[S32]
2-Naphthol	328.15	0.6456[S33]	118.50[S31]
1,4-Naphthoquinone	308.15	0.2264[S34]	111.2[S31]
naphthalene	308.15	29.23[S33]	110.0[S33]
p-Quinone	318.15	65.3424[S21]	82.02[S21]
Phenanthrene	308.15	0.053[S28]	155[S28]
Bipheny	308.15	4.28[S34]	132[S34]

Table S2 Molecular weight (M_w), critical temperatures (P_c), critical pressures (T_c), acentric factor (ω), and *Lennard-Jones* potential parameters of the substances.

Substances	M_W(g/mol)	T_c (K)	P_c(MPa)	ω	σ (Å)	ε/k (K)
CO_2	44.010[S13]	304.12[S13]	7.374[S13]	0.225[S13]	3.941[S13]	195.2[S13]
Ethane	30.070[S13]	305.32[S13]	4.872[S13]	0.099[S13]	4.443[S13]	215.7[S13]
Ethylene	28.054[S13]	282.34[S13]	5.041[S13]	0.087[S13]	4.163[S13]	224.7[S13]
Aspirin	180.16[S30]	762.9[S30]	3.28[S30]	0.817[S30]	6.961	565.1
Benzoic acid	122.12	751.0[S28]	4.47[S28]	0.6039[S28]	6.246	556.3
Naproxen	230.30[S29]	807[S29]	2.42[S29]	0.904[S29]	7.849	597.8
2-Naphthol	144.20	811.4[S31]	4.737[S31]	0.582[S31]	6.286	601.0
1,4-Naphthoquinone	158.16	792.2[S31]	4.12[S31]	0.575[S31]	6.533	586.8
Cholesterol	386.67[S32]	1168.23[S32]	4.155[S32]	0.950[S32]	7.415	865.4
Naphthalene	128.174[S13]	748.40[S13]	4.050[S13]	0.304[S13]	6.45[S6]	554.4[S6]
p-Quinone	108.09	747.3[S21]	5.002[S21]	0.424[S21]	6.007	553.6
Phenanthrene	178.233	890[S28]	3.25[S28]	0.429[S28]	7.350	659.3
Flouranthene	202.26	902.8[S31]	3.073[S31]	0.616[S31]	7.525	668.7
Biphenyl	154.211[S13]	773.0[S13]	3.38[S13]	0.404[S13]	6.922	572.6
Ethanol	46.069[S13]	513.92[S13]	6.148[S13]	0.649[S13]	4.530[S13]	362.6[S13]
Methanol	32.042[S13]	512.64[S13]	8.097[S13]	0.565[S13]	3.626[S13]	481.8[S13]
Ethyl acetate	88.106[S13]	523.20[S13]	3.830[S13]	0.361[S13]	5.205[S13]	521.3[S13]
Acetone	58.080[S13]	508.10[S13]	4.700[S13]	0.307[S13]	4.600[S13]	560.2[S13]
Cyclohexane	84.161[S13]	553.5[S13]	4.073[S13]	0.211[S13]	6.182[S13]	297.1[S13]
n-Pentane	72.150[S13]	469.7[S13]	3.370[S13]	0.252[S13]	5.784[S13]	341.1[S13]
Propane	44.097[S13]	369.83[S13]	4.248[S13]	0.152[S13]	5.118[S13]	237.1[S13]
Acetonitrile	41.053[S35]	545.5[S35]	4.83[S35]	0.327[S35]	5.471	404.1

Table S3 Binary interaction parameters of different systems in the PR-EOS.

Systems	T (K)	k_{12}	k_{13}	k_{23}
Aspirin(1) +ethanol(2) + CO_2 (3)	328.15	-0.973[S22]	0.2062[S22]	0.102[S22]
Aspirin(1)+methanol(2)+CO_2 (3)	318.15	-1.1140[S22]	0.2056 [S22]	0.066[S22]
Benzoic acid(1)+ethyl acetate(2) +CO_2 (3)	328.15	-0.4243	0.0450	0.1632[S36]
Naproxen(1)+acetone(2)+CO_2(3)	318.15	-1.2121	0.2230	0.0037[S30]
2-Naphthol(1)+cyclohexane(2)+CO_2(3)	328.15	0.0550	0.0792	0.1267[S37]
1,4-Naphthoquinone(1)+n-pentane(2) +CO_2(3)	308.15	0.1555	-0.0173	0.0510[S38]
Cholesterol(1)+ propane(2)+ Ethane(3)	318.15	0.3476	0.4422	0.001[S26]
Cholesterol(1)+ Acetone(2) + Ethane(3)	318.15	0.1660	0.4422	0.0500[S39]
Naphthalene(1) +CO_2(3)	308.15	-	0.095	-
Naphthalene(1) + Ethylene(3)	308.15	-	-0.010	-
p-Quinone(1)+CO_2(3)	318.15	-	0.1050	-
Aspirin(1)+ ethanol(2)+CO_2(3)	308.15	-0.7423	0.2086	0.077[S40]
Aspirin(1)+ acetone (2)+CO_2(3)	308.15	-0.2206	0.2086	0.008[S40]
Benzoic acid(1)+ n-pentane(2)+CO_2(3)	308.15	-0.3233	0.0324	0.0510[S38]
Benzoic acid(1)+ acetonitrile(2)+CO_2(3)	308.15	-0.0930	0.0324	0.065[S41]
Phenanthrene(1)+ n-pentane(2)+CO_2(3)	308.15	-0.0122	0.1125	0.0510[S38]
Phenanthrene(1)+ acetone(2) +CO_2(3)	308.15	-0.0069	0.1125	0.008[S40]
Flouranthene(1)+ n-pentane(2)+ CO_2(3)	308.15	0.0797	0.1374	0.0510[S38]
Flouranthene(1)+ acetone (2)+ CO_2(3)	308.15	0.1156	0.1374	0.008[S40]
Bipheny(1)+ n-pentane(2)+ CO_2(3)	308.15	-0.0962	0.0904	0.0510[S38]
Naphthalene(1)+ n-pentane(2)+ CO_2(3)	308.15	0.0142	0.095	0.0510[S38]

References

S1. M. McHugh, V. Krukonis, *Supercritical Fluid Extraction: Principles and Practice*, 2nd ed., Butterworth-Heinemann, Boston, 1994.

S2. H. F. Zhang, B. X. Han, Z. S. Hou, Z. M. Liu, *Fluid Phase Equilibr*. 2001, **179**, 131.

S3. Y. V. Tsekhanskaya, M. B. Iomtev, E. V. Mushkina, *Russ. J. Phys. Che*m. 1964, **38**, 1173.

S4. S. T. Chung, K. S. Shing, *Fluid Phase Equilibr*. 1992, **81**, 321.

S5. J. M. Prausnitz, R. N. Lichtenthaler, E. G. De Azevedo, *Molecular Thermodynamics of Fluid-Phase Equilibria*, 3rd ed., PTR Prentice Hall, Upper Saddle River, New Jersey, 1999.

S6. X. G. Zhang, B. X. Han, J. L. Zhang, H. P. Li, J. He, H. K. Yan, *Chem. Eur. J.* 2001, **7**, 19.

S7. J. M.Stubbs, D. D. Drake-Wilhelm, J. I. Siepmann, *J. Phys. Chem. B.* 2005, **109**, 19885.

S8. M. P. Allen, D. J. Tildesley, *Computer Simulation of Liquids*, Oxford University Press, Oxford, U. K., 1987.

S9. N. Metropolis, A. W. Rosenbluth, M. N. Rosenbluth, A. H. Teller, E. Teller, *J. Chem. Phys.* 1953, **21**, 1087.

S10. J. E. Lennard-Jones, *Proc. Phys. Soc.* 1931, **43**, 461.

S11. Y. Iwai, H. Uchida, Y. Koga, Y. Mori, Y. Arai, *Fluid Phase Equilibr.* 1995,**111**, 1.

S12. J. J. Nicolas, K. E. Gubbins, W. B. Streett, D. Tildesley, *J. Mol. Phys.* 1979, **37**, 1429.

S13. B. E. Poling, J. M. Prausnitz, J. P. O'Connell, *The Properties of Gases and Liquids*, 5th ed, McGraw-Hill, New York, 2000.

S14. I. Skarmoutsos, D. Dellis, J. Samios, *J. Chem. Phys.* 2007, **126**, 224503.

S15. K. Nakanishi, S. Okazaki, K. Ikari, T. Higuchi, H. Tanaka, *J. Chem. Phys.* 1982, **76**, 629.

S16. C. Rey, L. J. Gallego, L. E. Gonzalez , D. J. Gonzalez, *J. Chem. Phys*. 1992, **97**, 5121.

S17. D. Y. Peng, D. B. Robinson, *Ind. Eng. Chem. Fundam*. 1976, **15**, 59.

S18. Z. M. Liu, W. Z. Wu, B. X. Han, Z. X. Dong, G. Y. Zhao, J. Q. Wang, T. Jiang, G. Y. Yang, *Chem. Eur. J.* 2003, **9**, 3897.

S19. L. Gao, W. Z. Wu, Z. S. Hou, T. Jiang, B. X. Han, J. Liu, Z. M. Liu, *J. Phys. Chem. B.* 2003,**107**, 13093.

S20. G. A. M. Diepen, F. E. C. Scheffer, *J. Am. Chem. Soc.* 1948,**70**, 4085.

S21. P. Coutsikos, K. Magoulas, D. Tassios, *J. Chem. Eng. Data* 1997, **42**, 463.

S22. Z. Huang, Y. C. Chiew, W. D . Lu, S. Kawi, *Fluid Phase Equilibr*. 2005, **237**, 9.

S23. S. S. T. Ting, D. L. Tomasko, N. R. Foster, S. J. Macnaughton, *Ind. Eng. Chem. Res.* 1993, **32**, 1471.

S24. Q. S. Li, Z. T. Zhang, C. L. Zhong, Y. C. Liu, Q. R. Zhou, *Fluid Phase Equilibr*. 2003, **207**, 183.

S25. T. C. Mu, X. G. Zhang, Z. M. Liu, B. X. Han, Z. H. Li, T. Jiang, J. He, G. Y. Yang, *Chem. Eur. J.* 2004, **10**, 371.

S26. H. Singh, S. L. J. Yun, S. J. Macnaughton, D. L. Tomasko, N. R. Foster, *Ind. Eng. Chem. Res*. 1993, **32**, 2841.

S27. N. R. Foster, H. Singh, S. L. J. Yun, D. L. Tomasko, S. J. Macnaughton, *Ind. Eng. Chem. Res.* 1993, **32**, 2849.

S28. E. Bertakis, I. Lemonis, S. Katsoufis, E. Voutsas, R. Dohrn, K. Magoulas, D. Tassios, *J. Supercrit. Fluids* 2007, **41,** 238.

S29. S. S. T. Ting, D. L. Tomasko, N. R. Foster, S. J. Macnaughton, *Ind. Eng. Chem. Res.* 1993, **32**, 1482.

S30. K. W. Cheng, M. Tang, Y. P. Chen, *Fluid Phase Equilibr*. 2003, **214**, 169.

S31. P. Coutsikos, K. Magoulas, G. M. Kontogeorgis, *J. Supercrit. Fluids* 2003, **25**, 197.

S32. Z. Huang, S. Kawi, Y. C. Chiew, *J. Supercrit. Fluids* 2004, **30**, 25.

S33. M. Skerget, Z. Novak-Pintaric, Z. Knez, Z. Kravanja, *Fluid Phase Equilibr*. 2002, **203**, 111.

S34. W. J. Schmitt, R. C. Reid, *J. Chem. Eng. Data* 1986, **31**, 204.

S35. R. C. Reid, J. M. Prausnitz, B. E. Poling, *The Properties of Gases and Liquids*, 4th ed., McGraw-Hill, New York, 1987.

S36. A.Wyczesany, *Ind. Eng. Chem. Res.* 2007, **46**, 5437.

S37. M. C. Esmelindro, O. A. C. Antunes, E. Franceschi, G. R. Borges, M. L. Corazza, J. Vladimir Oliveira, W. Linhares, C. Dariva, *J. Chem. Eng. Data* 2008, **53**, 2050.

S38. J. W. Chen, W. Z. Wu, B. X. Han, L. Gao, T. C. Mu, Z. M. Liu, T. Jiang, J. M. Du, *J. Chem. Eng. Data* 2003, **48**, 1544.

S39. C.Yokoyama, H. Masuoka, K. Aral, S. Salto, *J. Chem. Eng. Data* 1985, **30**, 177.

S40. C. J. Chang, C. Y. Day, C. M. Ko, K. L. Chiu, *Fluid Phase Equilibr*. 1997, **131**, 243.

S41. M. Q. Hou, X. G. Zhang, B. X. Han, J. Y. Song, G. Liu, Z. F. Zhang, J. L. Zhang, *J. Chem. Phys.* 2008, **128**, 104510.